

Thin films of $\text{AgIn}_5(\text{S/Se})_8$ prepared in a two stage process

Sarah Messina¹ · Y. Rodríguez-Lazcano¹ · J. Campos² · Y. Peña³ ·
E. Barrios-Salgado¹

Received: 20 May 2016 / Accepted: 22 September 2016 / Published online: 19 October 2016
© Springer Science+Business Media New York 2016

Abstract $\text{AgIn}_5(\text{S/Se})_8$ thin films were prepared by sequential chemical deposition of $\text{In}_2\text{S}_3\text{-Ag}_2\text{Se}$ stack films and post-deposition thermal annealing in N_2 atmosphere. The formations of $\text{AgIn}_5\text{S}_{8-x}\text{Se}_x$ alloy was achievable through the post-deposition treatment at 350 and 400 °C. X-ray diffraction and energy dispersive X-ray analyses were performed on the samples. The direct optical band gap value E_g for the films was found to be as the order of 1.75 eV at room temperature. The photo-response measurements exhibited that $\text{AgIn}_5(\text{S/Se})_8$ thin films are photoconductive and p-type electrical conductivity of $6.6 \times 10^{-6} (\Omega \text{ cm})^{-1}$ and thermoelectric power of +18 $\mu\text{V/K}$.

1 Introduction

Chalcogenide ternary films of indium and silver have been reported with applications in optoelectronics and electronics devices [1–3]. Additionally, photovoltaic structure using AgIn_5S_8 has been obtained [2]. Furthermore, ternary AgIn_5Se_8 compound is an appropriate candidate for thermoelectric materials with many applications in the

conversion of thermal energy to electrical power [4, 5]. Moreover, metal chalcogenide semiconductors are promising as visible-light-driven photocatalysts. In view of this fact, AgIn_5S_8 displays high activity for the evolution of hydrogen [6].

AgIn_5S_8 has been obtained by different techniques such as thermal evaporation in one stage using AgIn_5S_8 single crystals as a source material [1], or two stages using thermal evaporation of precursor metals and sulfurization [7], microwave hydrothermal synthesis [8], pulsed laser deposition [9], growth solution techniques as chemical deposition [10, 11], one-pot synthesis [12] and low-temperature water bath deposition process to obtain AgIn_5S_8 nanocomposite [13]. AgIn_5Se_8 has been synthesized from the elementary components at 1200 K in a quartz evacuated ampoule and subsequently annealed at 820 K for 300 h [14]. Alloys of $\text{AgIn}_5\text{S}_{8-x}\text{Se}_x$ have been prepared by sintering stoichiometric mixtures of the binary compounds Ag_2S and Ag_2Se disposed at 773 K from the elements; and In_2S_3 and In_2Se_3 disposed at 1073 K from the elements, in evacuated and sealed silica ampoules at 1073 K and heated for 72 h at 1073 K [15]. Yiyun et al. [4] obtained a single phase of AgIn_5Se_8 by spark plasma sintering technique. Among the above mentioned methods, chemical bath deposition (CBD) is well known as a viable process to obtain large area and high quality semiconductor thin films with the advantages of simply, low cost and low energy consumption [16].

AgIn_5S_8 has been reported with *n*-type electrical conductivity and direct band gap of about 1.7 eV [17]. Vacuum evaporated AgIn_5S_8 thin films annealed in nitrogen at 450 and 600 K display energy band gap of 1.74 and 1.78 eV, respectively [18]. Qasrawi [19] obtained polycrystalline cubic AgIn_5S_8 samples, which exhibit direct allowed transitions and band gap energy of

✉ Sarah Messina
sarah.messina.uan@gmail.com

¹ Universidad Autónoma de Nayarit, Ciudad de la Cultura “Amado Nervo” S/N, C.P. 63155, Tepic, Nayarit, Mexico

² Instituto de Energías Renovables, Universidad Nacional Autónoma de México, C.P. 62580, Temixco, Morelos, Mexico

³ Facultad de Ciencias Químicas, Universidad Autónoma de Nuevo León, Av. Universidad S/N Ciudad Universitaria, C.P. 66451, San Nicolás de Los Garza, Nuevo León, Mexico

1.78 eV. Photoconductivity of the as-grown and nitrogen heat-treated AgIn_5S_8 films displays two recombination centers located at 66 and 16 meV [20]. Effects of temperature on the fundamental absorption edge produce a shift of the energy band gap from 1.78 to 1.73 eV as temperature boosts from 300 to 450 K. What is more, the fundamental absorption edge exhibited a temperature coefficient of -3.56×10^{-4} eV/K [21]. The carrier density of thermally deposited AgIn_5S_8 thin films increases from 1.74×10^{16} to 2.80×10^{19} cm^{-3} as the annealing temperature is raised from 350 to 450 K; and the Hall mobility decreases from a value of $16.7 \text{ cm}^2 \text{ V}^{-1} \text{ s}^{-1}$ at 350 K to $6.9 \text{ cm}^2 \text{ V}^{-1} \text{ s}^{-1}$ at 450 K [22]. Also, conductivity activation energies of 155 and 78 meV, in the temperature regions of 230–300 K and 90–220 K, respectively; and a density of localized states of $1.17 \times 10^{20} \text{ cm}^{-3} \text{ eV}^{-1}$, were reported [23]. On the other hand, previous work on ternary AgIn_5Se_8 compound and AgIn_5S_8 – AgIn_5Se_8 system have been focused in structural and compositional analysis [4, 14, 15]. Seebeck coefficients for spark plasma sintering AgIn_5Se_8 are negative, which indicates that the majority of charge carriers are electrons (*n*-type) [5]. In addition to this, single phase of AgIn_5S_8 displays a band gap of 1.11 eV [4, 5], whereas 1.22 eV is reported for $\text{Ag}_3\text{In}_5\text{Se}_9$ [17].

For this study, we have synthesized $\text{AgIn}_5(\text{S}/\text{Se})_8$ thin films on corning glass substrates using a two stage process which consist on sequential chemical deposition of In_2S_3 and Ag_2Se films, followed by thermal annealing in nitrogen atmosphere at 350 and 400 °C. Thin film formation was determined by X-ray diffraction (XRD). Compositional, optical and electrical properties of such thin films are also analyzed in this work.

2 Experimental details

2.1 Thin films deposition

2.1.1 In_2S_3 thin films

In_2S_3 thin films were obtained by CBD following the method previously reported by Lugo et al. [13] but changing the indium source. Reaction solution in this work was carried out using the following chemical reagents in the order described here: 10 mL of InCl_3 0.1 M, 2 mL of CH_3COOH 0.1 M, 16 mL of CH_3CSNH_2 1 M, and water to complete a volume of 100 mL. Glass substrates (Corning, 25 mm × 75 mm) were placed vertically into the beaker. Chemical deposition was carried out at 35 °C for 20 h, with this conditions the thickness of the films is 240 nm.

2.1.2 Ag_2Se thin films

Ag_2Se thin films were prepared using a reaction solution consisted on dissolving 100 mg of AgNO_3 in 10 mL water. Then 4 mL of 7.5 M of ammonia (aq.), 81 mL of deionized water and 5 mL of 0.1 M solution of Na_2SeSO_3 were mixed as described in [24]. Ag_2Se thin films were deposited at 10 °C during 30 min, the thickness of the films is (40 ± 3) nm.

2.1.3 In_2S_3 – Ag_2Se stacking process

In_2S_3 – Ag_2Se stacks were obtained by using sequential chemical bath of In_2S_3 and Ag_2Se . Ag_2Se thin films were deposited onto previously grown In_2S_3 layers. First, In_2S_3 thin films were grown on glass substrate as stated before. Subsequently, In_2S_3 films were immersed vertically into the beaker containing the solution to produce Ag_2Se thin films. The Ag_2Se deposition was carried out under the condition (time and temperature) mentioned above. Hence, In_2S_3 – Ag_2Se stacks were obtained.

2.2 Heat treatment

The In_2S_3 – Ag_2Se stack films were enveloped in Al foil and, subsequently, annealed in 1 Torr nitrogen atmosphere at 350 and 400 °C during 1 h, using a vacuum oven MTI-VBF-1200X. Film thickness measurements for In_2S_3 – Ag_2Se thin films after heating resulted as (270 ± 14) nm.

3 Characterization

X-ray diffraction (XRD) patterns were recorded on a Rigaku Ultima IV diffractometer with $\text{Cu-K}\alpha$ (1.5406 Å) radiation making grazing incidence of 1.0° with the sample plane. Such grazing incidence XRD (GIXRD) study helps to assess the structure and composition of the film along its thickness. An Oxford X-act energy dispersive X-ray spectrum (EDX) analyzer attached to a Hitachi-SEM SU1510 is used to analyze the chemical composition of the films. Optical transmittance (T) and specular reflectance (R) spectra of the films were recorded for film-side incidence with air and a front aluminized mirror as references on a UV–VIS–NIR V-670 JASCO spectrophotometer. The measured T and R data were used to evaluate the optical absorption coefficients (α) by considering multiple reflections within the thin film [25]. Pairs of silver-print electrodes 5 mm long at 5 mm separation applied on the film surface and dried at 60 °C for 30 min are used as contacts for the electrical characterization of the films. Keithley 230 programmable voltage source and Keithley 619 electrometer were utilized to study the photocurrent response of the films produced to different heat treatments. Each sample was stabilized in the dark in the measurement chamber. With a

bias (V) of 100 V across the electrodes (established previously as ohmic region), the current (I) in the sample was recorded at each 0.5 s for the first 20 s in the dark, the next 20 s under illumination and for the last 20 s after switching off the illumination. A tungsten-halogen ELH lamp provides an intensity of 1000 W/m^2 on the plane of the film. Electrical conductivity (σ) of the material of the different films is estimated from the current and voltage values, the electrode geometry and the film thickness. Films thickness was measured using an XP-200 Ambios Technology profilometer. The Seebeck voltage was measured by a microvoltmeter/Scanning thermometer Keithley 740, and the DC Power supply with two Peltier elements to establish a difference of temperature. This measurement was used to determined conductivity type of the films.

4 Results and discussion

4.1 Structural properties

Figure 1 shows XRD patterns of In_2S_3 thin films annealed in N_2 at (a) 350°C and (b) 400°C . We have observed in both films that XRD peaks remain in the same position as that in the standard powder pattern JCPDS- 01074-7284 corresponding to In_2S_3 of tetragonal structure with lattice

parameter values $a = 7.6172 \text{ \AA}$; $b = 7.6172 \text{ \AA}$; and $c = 32.3307 \text{ \AA}$, so the increment in temperature from 350 to 400°C does not suggest any structural transition.

Thermal annealing of $\text{In}_2\text{S}_3\text{-Ag}_2\text{Se}$ stack films at 350 and 400°C during 1 h produces a solid state reaction with the formation of the $\text{AgIn}_5(\text{S/Se})_8$ thin film as XRD patterns in Fig. 2a, b shown. The diffractogram shows XRD peaks matching well with the standard pattern of cubic AgIn_5S_8 with cell parameter $a = 10.825 \text{ \AA}$ (JCPDS-26-1477) and tetragonal AgIn_5Se_8 with cell parameter $a = 5.7740 \text{ \AA}$, $b = 5.7740 \text{ \AA}$ and $c = 11.6100 \text{ \AA}$ (JCPDS 26-1471). Diffraction peaks at $2\theta = 14.2^\circ$, 23.2° , 33.1° , 44.1° and 47.7° match with (111), (220), (311), (400), (511) and (440) planes from AgIn_5S_8 standard, respectively. On the other hand, the peaks at $2\theta = 26.83$, 38.1 and 44.37 match with (112), (202) and (220) planes from AgIn_5Se_8 standard, respectively. Peak at $2\theta = 24.9^\circ$ is associated with (110) plane of In_2Se_3 (JCPDS- 00-023-0294). XRD peaks remain unchanged with the increase in annealing temperature and, hence, we established 350°C as a proper temperature to obtain the ternary compound. To estimate the value of x in the $\text{AgIn}_2\text{S}_{8-x}\text{Se}_x$ alloy, we follow a method previously reported in Ref. [26] in which it is assumed a linear variation of inter-planar spacing d for the solid solution $\text{Sb}_2\text{S}_x\text{Se}_{3-x}$. This leads to the designation of the thin film in the cell structure as $\text{AgIn}_5\text{S}_{7.8}\text{Se}_{0.2}$.

Fig. 1 XRD patterns of In_2S_3 thin films heated at 350 and 400°C

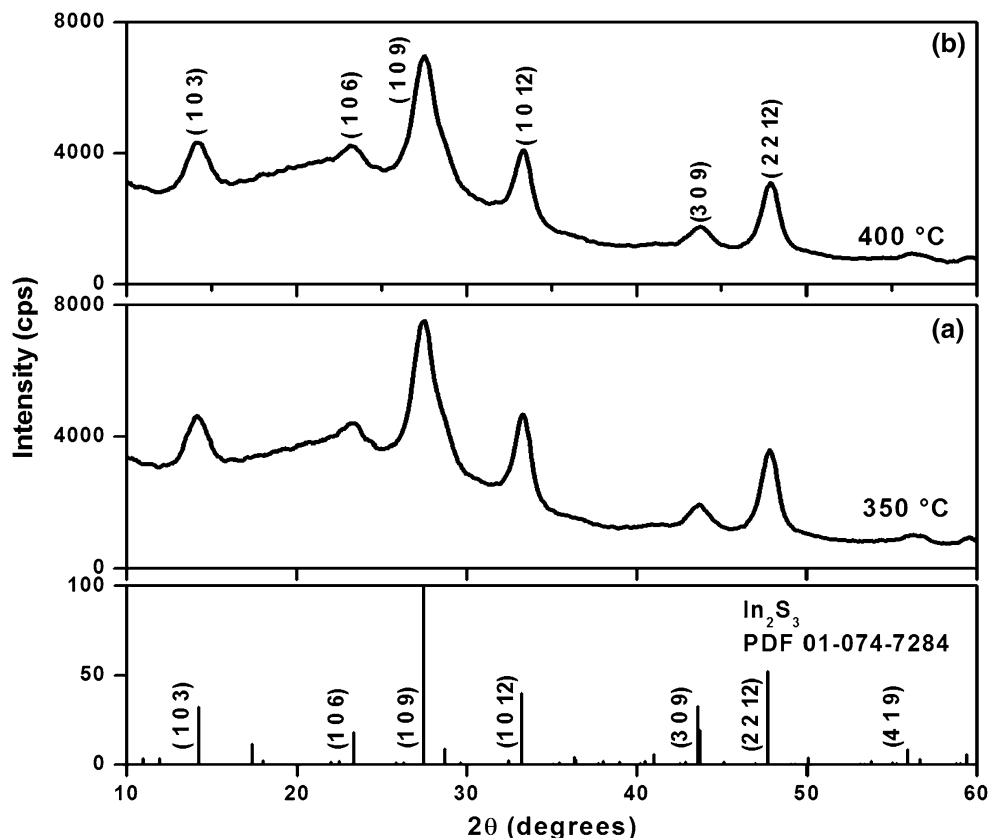
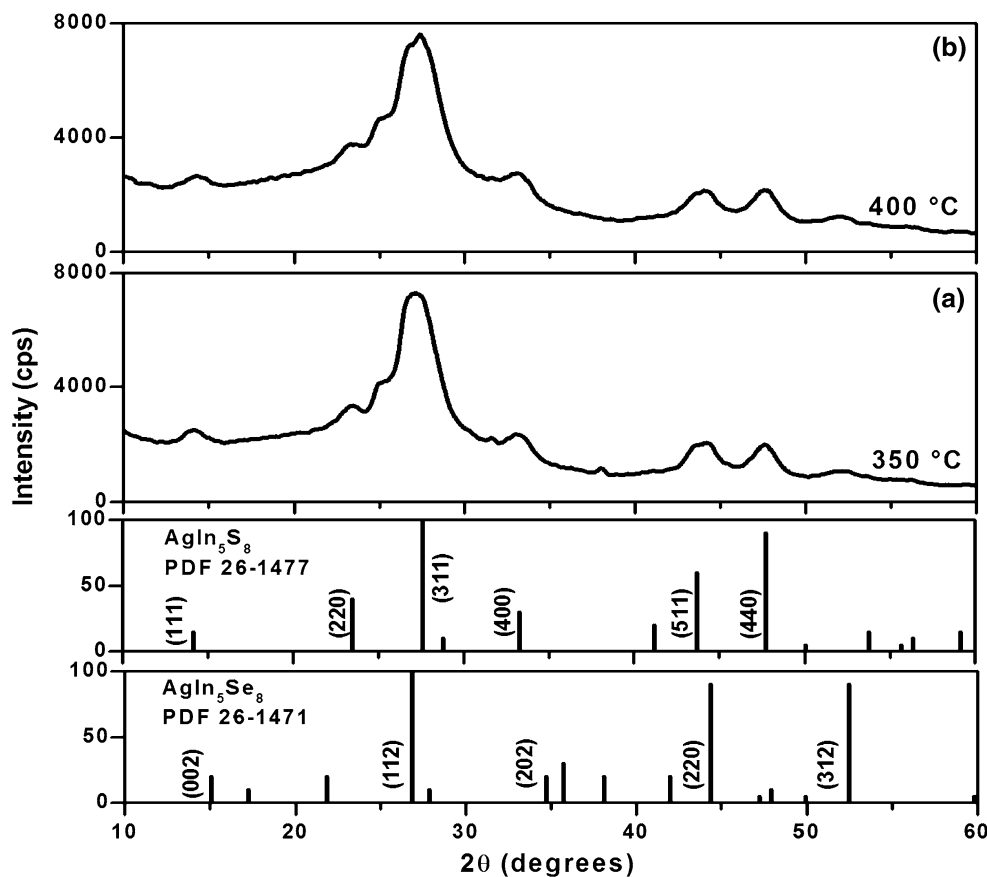


Fig. 2 XRD patters of In_2S_3 - Ag_2Se stack films heated at 350 and 400 °C



4.2 Chemical composition

The characteristic peaks of In-L_α at 3.286 keV and S-K_α at 2.307 keV; or In-L_α at 3.286 keV, Ag-L_α at 2.98 keV, Se-L_α at 1.379 keV and S-K_α at 2.307 keV are identified in the EDX spectra of In_2S_3 films or In_2S_3 - Ag_2Se stack films annealed at 350 °C, along with Si-K_α at 1.74 keV arising from the substrate. Figure 3 shows the EDX spectrum of $\text{AgIn}_5(\text{S/Se})_8$ thin film. The composition of In_2S_3 films correspond to weight percentage of: $\text{In} = 72.9\%$ and $\text{S} = 27.1\%$. This result indicated that the composition of the film is close to the stoichiometric formula of In_2S_3 , where $\text{In}:\text{S}$ ratio is 2:3. Thin films of $\text{AgIn}_5(\text{S/Se})_8$ present the following results: $\text{Ag} = 16.4\%$, $\text{In} = 59.9\%$, $\text{S} = 20.6\%$ and $\text{Se} = 2.9\%$. Such S-rich films are in agreement with the results reported by Haeuseler and coworker on the system $\text{AgIn}_5\text{S}_{8-x}\text{Se}_x$ ($0 < x < 8$), where 11 different compositions were found [15]. Thus, according to XRD and EDX results, we propose that the solid state reaction produced by the thermal annealing of In_2S_3 - Ag_2Se stack films results on the formation of $\text{AgIn}_5\text{S}_{7.8}\text{Se}_{0.2}$ alloy thin films. EDX analyses show that chemical composition is homogeny along the samples. The errors in the data were evaluated to be about 5%.

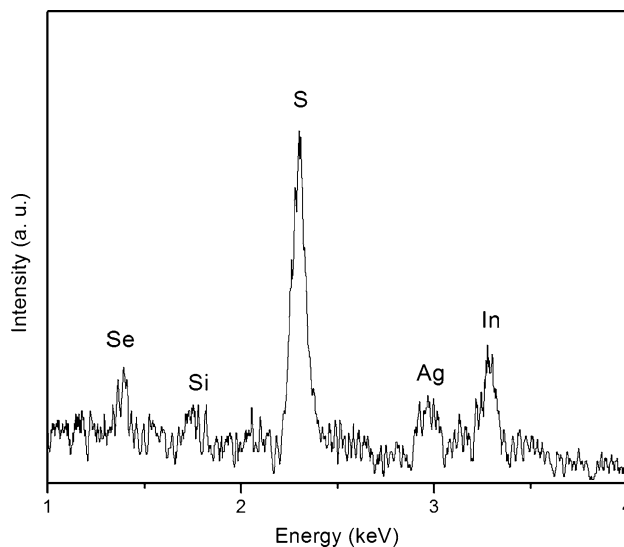


Fig. 3 EDX spectrum of In_2S_3 - Ag_2Se thin films heated at 350 °C

4.3 Optical properties

Optical properties were recorded in the range between 250 and 2500 nm. Figure 4 illustrates the optical transmittance (T) and the specular reflectance (R) for In_2S_3 and In_2S_3 - Ag_2Se thin films heated at 350 °C.

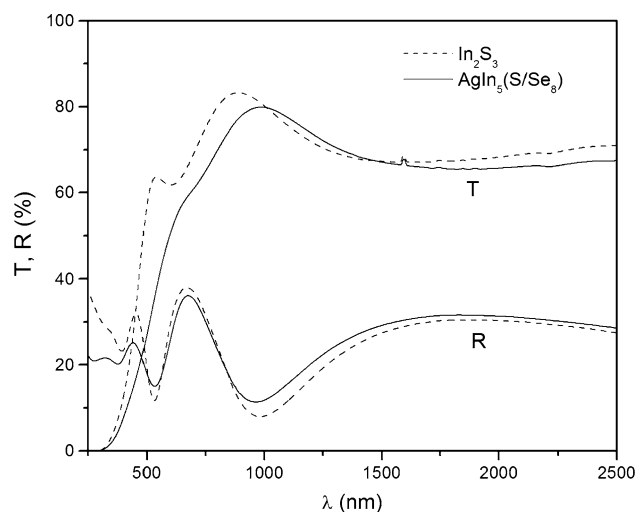


Fig. 4 Transmittance (T) and reflectance (R) spectra for In_2S_3 and $\text{AgIn}_5(\text{S/Se})_8$ samples after heating at $350\text{ }^\circ\text{C}$

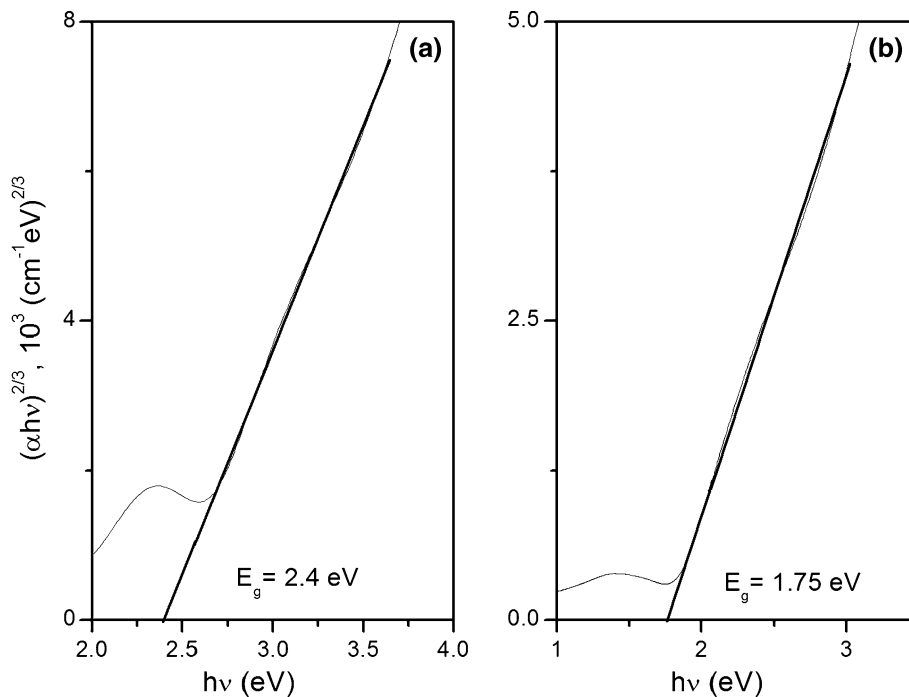
Optical absorption coefficient (α) as a function of the photon energy ($h\nu$) was estimated from the transmittance (T) and reflectance (R) spectra data; and film thickness (d) measurements according to the following equation [25]:

$$\alpha = \frac{1}{d} \ln \left\{ \frac{(1-R)^2}{2T} + \left[\left(\frac{(1-R)^2}{2T} \right)^2 + R^2 \right]^{\frac{1}{2}} \right\} \quad (1)$$

The band gap (E_g) was calculated using the relationship:

$$\alpha h\nu = A(h\nu - E_g)^n \quad (2)$$

Fig. 5 Optical band gap for **a** In_2S_3 and **b** $\text{AgIn}_5(\text{S/Se})_8$ thin films



were A is a constant as a function of the transition probability.

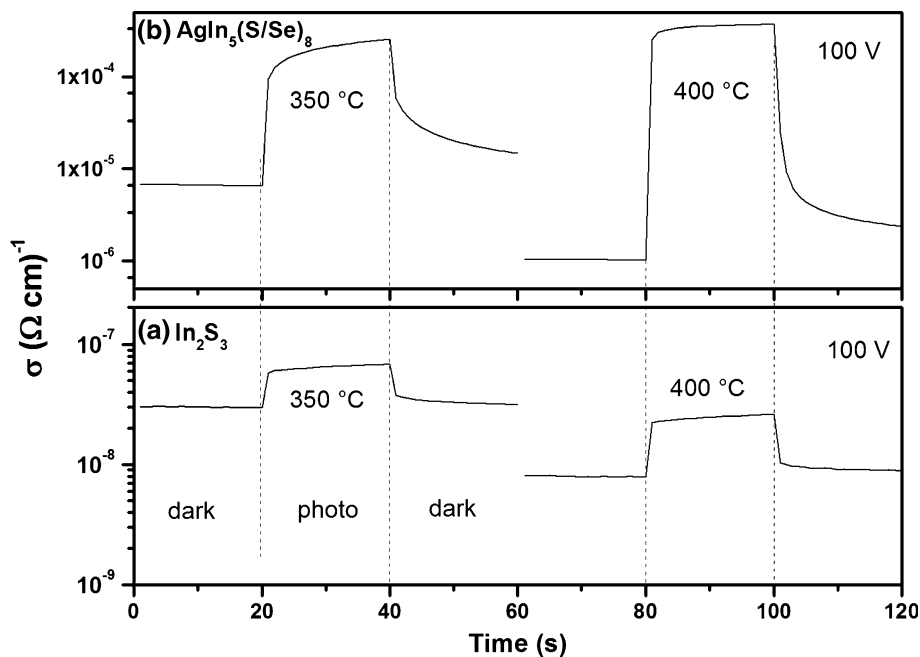
Plot of $(\alpha h\nu)^{2/3}$ versus $h\nu$ was used to calculate the value of energy band gap by adjusting the linear part of the curve, as shown in Fig. 5a. Straight line region in this plot indicates that the absorption edge corresponds to a direct forbidden electronic transition. The value of E_g was obtained when the adjusting line tends to zero. For In_2S_3 layer heated at $350\text{ }^\circ\text{C}$ $E_g = (2.4 \pm 0.4)\text{ eV}$, which corresponds to that value reported in literature for In_2S_3 thin films [27].

Plot of $(\alpha h\nu)^{2/3}$ versus $h\nu$ is given in Fig. 5b for $\text{AgIn}_5(\text{S/Se})_8$ thin film. The energy band gap E_g was calculated according to the Eq. (2). The linearity of plot $(\alpha h\nu)^{2/3}$ versus $h\nu$ indicates that the absorption edge corresponds to a direct forbidden transition. The E_g value obtained was $(1.75 \pm 0.6)\text{ eV}$. Only values for the AgIn_5S_8 ($1.74\text{--}1.78\text{ eV}$) and AgIn_5Se_8 (1.1 eV) has been reported previously [4, 5, 11, 18, 19]. We suggest that the band gap value is close to the AgIn_5S_8 because the small quantity of selenium; in agreement with XRD and EDX results. The values of the optical absorption coefficient, $\alpha > 10^4\text{ cm}^{-1}$, in addition to the optical band gap value allow us to consider the $\text{AgIn}_5(\text{S/Se})_8$ film as a promising candidate for solar cell applications.

4.4 Electrical properties

Photo-response measurements of In_2S_3 and $\text{In}_2\text{S}_3\text{--Ag}_2\text{Se}$ thin films annealed at $350\text{ }^\circ\text{C}$ in N_2 are given in Fig. 6. The

Fig. 6 Photo-response measurements of In_2S_3 and $\text{In}_2\text{S}_3\text{-Ag}_2\text{Se}$ thin films heated at **a** 350 °C and **b** 400 °C



electrical conductivity of In_2S_3 thin films heating at 350 °C is $\sigma_{\text{dark}} = 3.7 \times 10^{-8} (\Omega \text{ cm})^{-1}$, when the film is heated at 400 °C the conductivity is at the same order of magnitude as shown in Fig. 6a, this result is in agreement with the value reported previously for thin films by chemical deposition [28]. The $\text{In}_2\text{S}_3\text{-Ag}_2\text{Se}$ thin films annealing at 350 °C exhibit a value of $\sigma_{\text{dark}} = 6.6 \times 10^{-6} (\Omega \text{ cm})^{-1}$ that is very similar to the stack films heating at 400 °C, as observed in Fig. 6b. This value is more than two orders of magnitude higher than In_2S_3 thin films, as expected, due to silver and selenide incorporation in the formation of $\text{AgIn}_5(\text{S/Se})_8$. Thin films of In_2S_3 heated at 350 °C shows a value of photo-conductivity (σ_{ph}) of $6.8 \times 10^{-8} (\Omega \text{ cm})^{-1}$. Additionally, $\text{AgIn}_5(\text{S/Se})_8$ presents a value of σ_{ph} of $2.5 \times 10^{-4} (\Omega \text{ cm})^{-1}$, two orders of magnitude higher than in the dark. The errors in the data were evaluated to be 2–5 %.

The thermoelectric potential (V) at the cold end with respect to the hot end of the semiconductor subjected to a temperature difference ΔT was measured. Figure 7 shows the result for $\text{AgIn}_5(\text{S/Se})_8$ alloy produced from $\text{In}_2\text{S}_3\text{-Ag}_2\text{Se}$ stack films heated at 400 °C. The value of Seebeck coefficient is $+(18.7 \pm 0.9) \mu\text{V/K}$, so that suggesting that the film is slightly of p-type conductivity. Materials can be obtained either p-type or n-type, depending on growth conditions, stoichiometry and post-deposition thermal annealing. For instance, AgInSe_2 shows both n-type and p-type conductivity depending on particular growth conditions [29]. AgInSe_2 p-type films have been obtained by post-deposition thermal annealing under selenium atmosphere [30]. On the other hand, AgIn_5S_8 and AgIn_5Se_8 have been reported in the literature with n-type conductivity

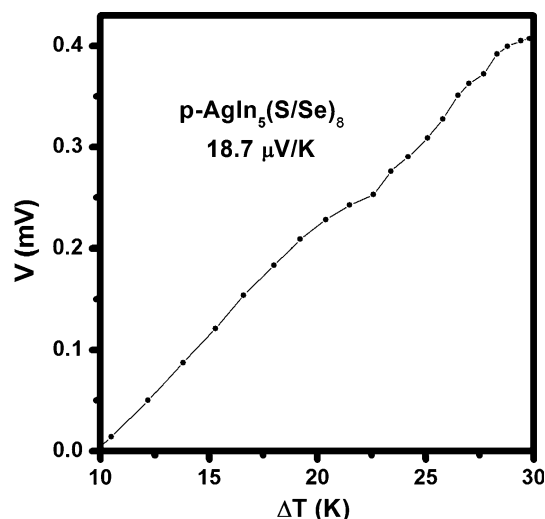


Fig. 7 Thermoelectric potential (V) versus temperature difference (ΔT) of $\text{AgIn}_5(\text{S/Se})_8$ produced from $\text{In}_2\text{S}_3\text{-Ag}_2\text{Se}$ stack films heated at 400 °C

[5, 17]. In this work we reported a new methodology for the formation of $\text{AgIn}_5(\text{S/Se})_8$ with p-type conductivity. We suggest that the incorporation of selenium in $\text{AgIn}_5(\text{S/Se})_8$ samples might be seen as a similar process to the post-deposition annealing under Se pressure in AgInSe_2 films [30]. The incorporation of selenium may lead to the formation of interstitial intrinsic defects that contribute to the p-type conductivity. P-type conductivity is desired for the absorber layer because of the heterojunction partner availability and the longer minority carrier diffusion length of electrons.

5 Conclusions

The films of $\text{AgIn}_5(\text{S/Se})_8$ were obtained on glass substrates by annealing at 350–400 °C in nitrogen atmosphere chemically deposited $\text{In}_2\text{S}_3\text{--Ag}_2\text{Se}$ stack films. The formation of the $\text{AgIn}_5\text{S}_{7.8}\text{Se}_{0.2}$ has been established on the basis of XRD and EDX results. The films have direct optical band gap of 1.75 eV and optical absorption coefficient of 10^4 cm^{-1} . Samples are photoconductive with p-type electrical conductivity (in dark) of $6.6 \times 10^{-6} (\Omega \text{ cm})^{-1}$. The Seebeck effect shows a value of +18 $\mu\text{V/K}$. The optical band gap, electrical conductivity and the photoconductivity of these materials fulfil the basic requirements for their integration into photovoltaic structures.

Acknowledgments We acknowledge the financial support of CONACYT through Project 229711, CONACYT-LIFYCS-123122 and CeMIE-Sol project 35 for using SEM and XRD. The authors strongly appreciate the technical assistance of Patricia Altuzar Coello and Oscar Gómez Daza from IER-UNAM, for XRD measurements and technical assistance, respectively. Student Adriana Gómez was involved in sample preparation.

References

1. A.F. Qasrawi, T.S. Kayed, I. Ercan, *Mater. Sci. Eng. B* **113**, 73 (2004)
2. I. Konovalov, L. Makhova, R. Hesse, R. Szargan, *Thin Solid Films* **493**, 282 (2005)
3. L. Makhova, I. Konovalov, R. Szargan, *Phys. Status Solidi A* **201**, 308 (2004)
4. L. Yiyun, M. Qingsen, C. Jiaolin, S. Weiwei, G. Yulan, *Procedia Eng.* **27**, 151 (2012)
5. J.L. Cui, Y.Y. Li, Y. Deng, Q.S. Meng, Y.L. Gao, H. Zhou, Y.P. Li, *Intermetallics* **31**, 217 (2012)
6. D. Chen, J. Ye, *J. Phys. Chem. Solids* **68**(12), 2317 (2007)
7. L. Makhova, R. Szargan, I. Konovalov, *Thin Solid Films* **472**, 157 (2005)
8. Z. Wenjuan, L. Danzhen, S. Meng, S. Yu, C. Zhixin, X. Guangcan, F. Xianzhi, *J. Solid State Chem.* **183**, 2466 (2010)
9. I.V. Bodnar, V.F. Gremenok, *Thin Solid Films* **487**, 31 (2005)
10. C. Kong-Wei, H. Chao-Ming, P. Guan-Ting, C. Wen-Sheng, L. Tai-Chou, C.K. Yang, *J. Photochem. Photobiol. A* **190**, 77 (2007)
11. C. Kong-Wei, W. Sheng-Chih, *Sol. Energy Mater. Sol. Cells* **93**, 307 (2009)
12. L. Xiangqing, W. Lei, W. Dailong, K. Shizhao, M. Jin, *Mater. Res. Bull.* **48**, 286 (2013)
13. S. Lugo, Y. Peña, M. Calixto-Rodríguez, C. López-Mata, M.L. Ramón, I. Gómez, A. Acosta, *Appl. Surf. Sci.* **263**, 440 (2012)
14. I.A. Ivashchenko, L.D. Gulay, O.F. Zmiy, I.D. Olekseyuk, *J. Alloys Compd.* **427**, 101 (2007)
15. H. Haeuseler, E. Elitok, A. Memo, A. Osnowsky, *Mater. Res. Bull.* **36**, 737 (2001)
16. G. Hodes, *Chemically Solution Deposition of Semiconductor Films*, 1st edn. (Marcel Dekker Inc., New York, 2003), pp. 32–33
17. O. Madelung, *Semiconductors Other than Group IV Elements and III–V Compounds*, 1st edn. (Springer, Berlin, 1992), pp. 50–52
18. A.F. Qasrawi, *J. Alloys Compd.* **455**, 295 (2008)
19. A.F. Qasrawi, *Thin Solid Films* **516**, 1116 (2008)
20. A.F. Qasrawi, T.S. Kayed, E. Ismail, *J. Alloys Compd.* **508**, 380 (2010)
21. A.F. Qasrawi, *Thin Solid Films* **519**, 3768 (2011)
22. A.F. Qasrawi, T.S. Kayed, E. Filiz, *Solid State Commun.* **151**, 615 (2011)
23. A.F. Qasrawi, *Thin Solid Films* **519**, 6583 (2011)
24. K. Bindu, M.T.S. Nair, T.K. Das Roy, P.K. Nair, *Electrochem. Solid State Lett.* **6**, G195 (2006)
25. D.K. Schroder, *Semiconductor Materials and Device Characterization*, 2nd edn. (Wiley, New York, 1990), pp. 596–597
26. M. Calixto-Rodríguez, H. Moreno-García, M.T.S. Nair, P.K. Nair, *J. Solid State Sci. Technol.* **2**, Q69 (2013)
27. M.G. Sandoval-Paz, M. Sotelo-Lerma, J.J. Valenzuela-Jauregui, M. Flores-Acosta, R. Ramírez-Bon, *Thin Solid Films* **472**, 5 (2005)
28. S. Lugo-Loredo, Y. Peña-Méndez, M. Calixto-Rodríguez, S. Messina-Fernández, A. Alvarez-Gallegos, A. Vázquez-Dimas, T. Hernández-García, *Thin Solid Films* **550**, 110 (2014)
29. D. Abdel-Hady, A.M. Salem, *Phys. A Stat. Theor. Phys.* **242**, 141 (1997)
30. K. Yoshino, *Phys. B Condens. Matter* **302**, 349 (2001)